Stability and electronic properties of hydrogenated C_3B structure

Tong Liu[1], Dong Fang[1], Jie Ma[2], Qun Chao Fan[1,*]

[1,*]School of Science, Key Laboratory of High Performance Scientific Computation, Xihua University, Chengdu 610039, China
[2] State Key Laboratory of Quantum Optics and Quantum Optics Devices, Laser Spectroscopy Laboratory, College of Physics and Electronics Engineering, Shanxi University, Taiyuan 030006, China

Abstract: Experimental and theoretical studies show that two-dimensional (2D) materials have great potential applications in the fields of optoelectronics, semiconductors and spintronic devices. Based on the First Principles, the stability, band structure, electronic properties and optical properties of hydrogenated C_3B, a new graphene like two-dimensional (2D) material, are studied in this paper. The results show that: firstly, with the increase of hydrogenation degree, the sp^2 orbital hybridization in C_3B structure gradually transits to a more stable sp^3 mode, and the valence band energy near the Fermi level decreases; Secondly, adsorbed H atoms can regulate the bandgap of C_3B. When the number of adsorbed H is even, C_3B structure behaves as a semiconductor, and meanwhile the bandgap increases. When H atoms is odd, C_3B is easy to show metallicity; Finally, the main absorption peak of the optical absorption spectrum decreases first and then increases with the increase of H concentration. The law of the secondary absorption peak is opposite to the main peak. When the ratio of hydrogenation is 50%, an obvious secondary absorption peak appears. This study confirms that hydrogenation is an effective way to regulate the electronic properties of materials, which can expand the application of 2D material C_3B in optoelectronic devices.

Keywords: First Principles, hydrogenated C_3B, electronic properties

1. Introduction

Over the past decade, the unique physical, electrical and optical characteristics of 2D materials, present specific opportunities in electronic and optoelectronic devices, such as transistors, electronic devices, photodetectors, light-emitting diodes, and energy storage[1-4]. The superlative properties of single-layer graphene have inspired aggressive exploration of other 2D materials. Up to now, the 2D material family is developing rapidly, covering superconducting materials (FeSe、$NbSe_2$)[5,6], metal materials (bilayer Borophene)[7-9], semiconductor materials (transition metal

* Corresponding authors at: School of Science, Xihua University, Chengdu 610039, China.
E-mail address: fanqunchao@mail.xhu.edu.cn

chalcogenides, TMDCs),[10-12] insulators (h-BN)[13,14] and so on. However, due to intrinsic characteristics of unitary 2D materials, its applications are limited in some aspects. For example, graphene has zero intrinsic band gap, which limits its application in semiconductor integrated materials, and monolayer borophene is prone to oxidative instability.[7,15] Therefore, it is very urgent to explore new multifunctional 2D materials with appropriate bandgap. To this end, on the one hand, many methods have been proposed to modulate the electronic properties of graphene with varying degrees of success, but graphene is still far away from the practical application in electronic equipment,[16] on the other hand, people are also actively looking for a variety of new 2D materials to expand the application range. In recent years, graphene-like materials with quasi-two-dimensional honeycomb structures have attracted extensive attention. The band structures and strain characteristics of C_3N explain its application in short channel electronic devices.[17,18] In addition, the prepared N-containing h2D-C_2N (holey 2D C_2N) may be a basic material for the future development of multifunctional 2D crystals.[19] Therefore, the application potential of hexagonal C_3B, a 2D semiconductor with moderate bandgap, cannot be ignored in the optoelectronics field.

The common methods to regulate the electronic properties of materials include external field regulation, construction of heterostructures, surface chemical modification and so on. Previous studies have shown that the band gaps of monolayer GeS, WS_2 and MoS_2 are rather sensitive to external electric field, and the semiconductor to metal transition can even occur under the action of external field;[20-22] The week interlayer coupling in 2D van der Waals heterojunctions, which can not only induce new properties, such as bandgap opening in graphene,[23-25] semiconductor band alignment,[26], charge separation and enhancing the photoactivity,[27,28], but also preserve the intrinsic properties of corresponding 2D materials. With atomic-scale thickness, 2D nanomaterials have an extremely high specific surface area, and therefore provide an ideal platform for modulating intrinsic physical properties by surface modification.[29] Surface chemical modification can not

only adjust the intrinsic physical properties, but also maintain the relative independence of the two-dimensional material lattice structure. The common methods include doping, adsorption and structural defects. For example, the introduction of 3d transition metals Fe and Co can synergistically optimize the electronic structure of the carbon nanotubes, and then promote the HER;[30] The study of monolayer SnO_2 and $ZnSe_2$ shows that surface distortion is shown to endow them with a unique electronic structure and excellent structural stability, thus determining their enhanced photoconversion efficiency and photostability.[31,32] There are many types of surface chemical modification, including non-metallic and transition metal elements, hydroxyl and carboxyl groups, as well as water and organic macromolecules.[33-35] Hydrogen, as the simplest element, generally appears as an electron donor when incorporated into the external lattice framework. The results show that hydrogenation has been successfully used to regulate the carrier concentration in bulk materials such as VO_2 and TiS_2;[36,37] After semi hydrogenation, the magnetic and electronic properties of graphitic BN are largely changed.[38] In a word, when studying the influence of chemical modification on the surface electronic properties of 2D materials, on the one hand, the type of functional groups should be considered, and on the other hand, the adsorption ratio should also be paid attention to.

Here, our research is based on First-Principle, hydrogen atoms as adsorbed atoms, and six different configurations of hydrogenation degree (including weak, semi, strong and full hydrogenation) are considered in order to comprehensively explore the effects of hydrogenation on the electronic properties of C_3B. Firstly, we design all possible configurations of hydrogen atoms adsorbed on the surface of C_3B, a total of 51. The most stable configuration corresponding to each degree of hydrogenation is determined according to the adsorption energy and phonon dispersion spectrum. Secondly, the stability and electronic properties of six hydrogenated C_3B are investigated in detail. Especially, we studied the role of hydrogen atoms on C_3B and if its band gap can be tuned by changing with the number of hydrogen atoms. In addition, we further analyzed the bonding information according to the density of

states (DOS) to determine the orbital electron contribution near the Fermi level. Finally, with the purpose of providing more information as possible, we calculate the optical spectrum of the six hydrogenated C_3B monolayer. Our present study tries to provide a simple and effective route to tune the electronic properties of monolayer C_3B over a wide range and eventually expand its application in the semiconductor field.

2. Method

All calculations are performed within the CASTEP code, which is based on density functional theory (DFT) and plane-wave pseudopotential method.[39,40] We choose the projector-augmented-wave (PAW) pseudopotentials to handle with the effect of core electrons and ions in calculations.[41] The generalized gradient approximation (GGA) of Perdew, Burke, and Ernzerhof (PBE) is chosen as exchange-correlation functional,[42] which is used to optimize the structure. During the structure optimization, the lattice constants and atomic internal coordinates are fully relaxed. The optimization will terminate if the force convergence criterion of 0.01 eV/Å is satisfied. The energy is converged to 10^{-5} eV per atom. A plane-wave basis with a kinetic energy cutoff of 550 eV was adopted. Vacuum space of 20 Å is enough to avoid the interlayer interaction. The Brillouion-Zone (BZ) integration was performed using the Monkhorst-pack sampling scheme with a grid of 7 x 7 x 1 k-points during configuration relaxation. The phonon dispersion spectrum is calculated by linear response method. The calculation formula of adsorption energy is as follows:

$$E_{Ads} = \frac{E_{Hyd} - E_{C_3B} - N_H \times E_H}{N_H}, \quad (1)$$

where the E_{Hyd}, E_{C_3B}, E_H and N_H represent total energy of hydrogenated C_3B, initial monolayer C_3B, an isolated hydrogen atom, and the number of adsorbed hydrogen atoms respectively. The larger the negative E_{Ads} value, the more energetically stable the structure is.

So far, six stable hydrogenated structures of C_3B have been obtained. These

structures correspond to two types of BZ. The grid of $5 \times 7 \times 1$ and $7 \times 7 \times 1$ k-points were adopted during electronic property calculation. All properties of these stable structures are calculated by hybrid density functional HSE06 (Heyd-Scuseria-Ernzerhof) method.[43].

$$\varepsilon(\omega) = \varepsilon_i(\omega) + i\varepsilon_i(\omega), \tag{2}$$

$$\alpha(E) = \frac{4\pi e}{hc}\left(\frac{\sqrt{(\varepsilon_1^2+\varepsilon_2^2)}-\varepsilon_1}{2}\right)^{\frac{1}{2}}, \tag{3}$$

The frequency dependent dielectric function and optical absorption coefficient are respectively expressed.

3. Results and Discussion

3.1 Stability of monolayer C_3B modified by hydrogen

C_3B, a fully flattened graphene-like structure, exhibits a six-membered ring which is formed by π bonds between C atoms, and the hybridization between C and H is carried out in the way of sp^2. The primitive cell of monolayer C_3B crystal contains six carbon atoms, as shown in Fig. 1(a). We're just going to hang H on top of C. In order to facilitate the description of the adsorption position, C atoms in Fig. 1(a) are marked with yellow English letters. The cell of this primitive C_3B contains a total of six C atoms. Hanging H atoms means hydrogenation. Hydrogenation can break the symmetry of the original structure and the bonding mode between atoms, which is expected to explore the novel photoelectric properties of C_3B structure.[44]. Up to six H atoms can be suspended in the cell of primitive C_3B. Obviously, the more H atoms are hung, the stronger the degree of hydrogenation will be. Hanging an H atom is said to be 12.5% hydrogenated. As the number of suspended H atoms increases from 1 to 6, the hydrogenation degree increases from 12.5% to 100% (the hydrogenation degree is saturated). There may be different adsorption sites in the same hydrogenation degree, and different adsorption sites may also have different arrangements. Taking all the

adsorption configurations into consideration, we designed a total of 51 structures for adsorbing H atoms. In other words, when the amount of adsorbed H atoms are 1, 2, 3, 4, 5 and 6, the corresponding hydrogenated configuration quantity are 1, 6, 9, 16, 10 and 8, respectively. Any configuration is named H_y^x-(C_3B), where x is 1, 2, 3, 4, 5 and 6, representing the number of adsorbed hydrogen atoms; y is α, β, γ, δ, ε, ζ, η, θ, ι, κ, λ, μ, ν, ξ, o and π，meaning different adsorption configurations with the same adsorption degree.

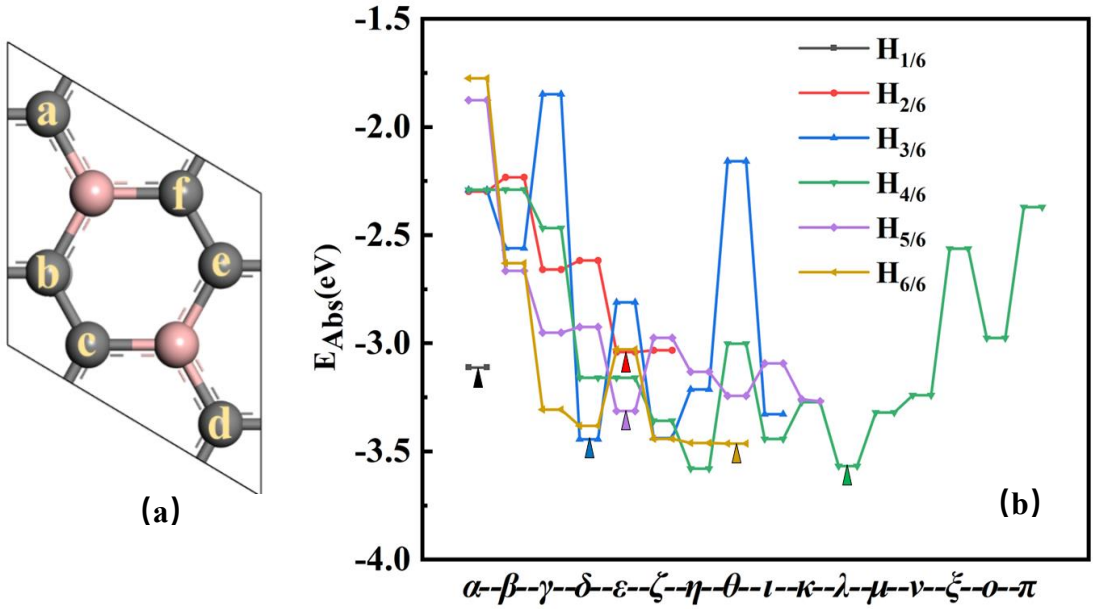

Fig. 1. (a) C_3B primary cell; (b) the adsorption energy of 51 hydrogenated structures, where x/6 (x=1, 2, 3, 4, 5, 6) represents the number of hydrogen atoms adsorbed.

Next, we performed structural relaxation on the above 51 configurations and calculated the E_{Ads} of each configuration in order to determine the most stable configuration that may appear at the same degree of hydrogenation. The E_{Ads} reflects the adsorption capacity of C_3B to H atoms and the stability of adsorption structure. Fig. 1(b) shows the adsorption energy of 51 hydrogenation configurations, in which the broken line diagram of the same color corresponds to the E_{Ads} of the same hydrogenation degree. The triangle position of each broken line indicates the lowest adsorption energy under the same hydrogenation degree. The results of theoretical calculation show that the adsorption energy of all structures is negative, that is to say, the adsorption process of all hydrogen atoms is exothermic. In addition,

the lower the adsorption energy is, the more heat will be released in the adsorption process, the stronger the stability of the adsorption structure becomes.

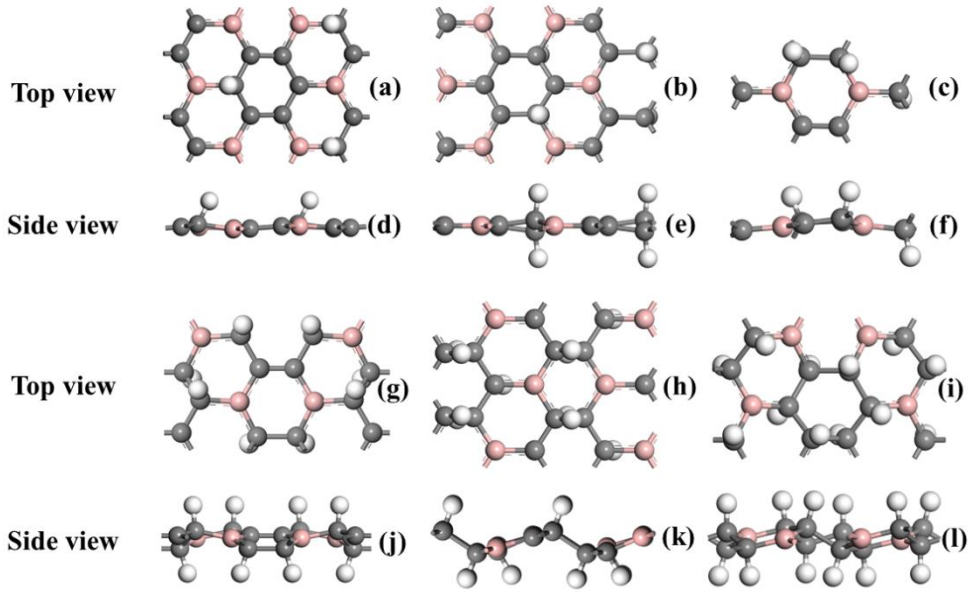

Fig. 2. Six stable hydrogenation configurations. (a-f) represents top and side views of H_{α}^{1}-*(C₃B)*, H_{ε}^{2}-*(C₃B)* and H_{δ}^{3}-*(C₃B)*; (g-l) represents top and side views of H_{λ}^{4}-*(C₃B)*, H_{ε}^{5}-*(C₃B)* and H_{θ}^{6}-*(C₃B)*.

Table 1. Adsorption sites and orientations of hydrogen atoms in six stable hydrogenation configurations.

Configuration \ Site	a	B	C	d	e	f
H_{α}^{1}-*(C₃B)*	up					
H_{ε}^{2}-*(C₃B)*	up	Down				
H_{δ}^{3}-*(C₃B)*	up	Down	Down			
H_{λ}^{4}-*(C₃B)*	Up	Down	Down	up		
H_{ε}^{5}-*(C₃B)*	Up	Down			up	down
H_{θ}^{6}-*(C₃B)*	Up	Down	Down	up	up	down

Obviously, for the same degree of hydrogenation, the site marked by the triangle corresponds to the most stable hydrogenation configuration at the same adsorption concentration. For instance, the blue line represents the adsorption energy of 9 configurations in the case of adsorption of three hydrogen atoms. It is easy to judge that the configuration corresponding to the lowest position of the adsorption energy is H_{δ}^{3}-(C_3B). Therefore, H_{δ}^{3}-(C_3B) is the most stable spatial configuration when the H adsorption concentration is 50%. We have identified six stable adsorption

configurations. According to the number of adsorbed hydrogen atoms, each stable adsorption configuration is named as: H_{α}^{1}-(C_3B)、H_{ε}^{2}-(C_3B)、H_{δ}^{3}-(C_3B)、H_{λ}^{4}-(C_3B)、H_{ε}^{5}-(C_3B) and H_{θ}^{6}-(C_3B). The top and side views of the six stable configurations are shown in Fig. 2. In order to facilitate a more intuitive understanding, combined with the C atom label in Fig. 1(a), we also give the sites and orientations of hydrogen atom adsorption. As shown in Fig. 2, the adsorption sites and orientations are represented by letters of C atom labels (a-f) and orientations (Up and Down), respectively (shown in Table 1).

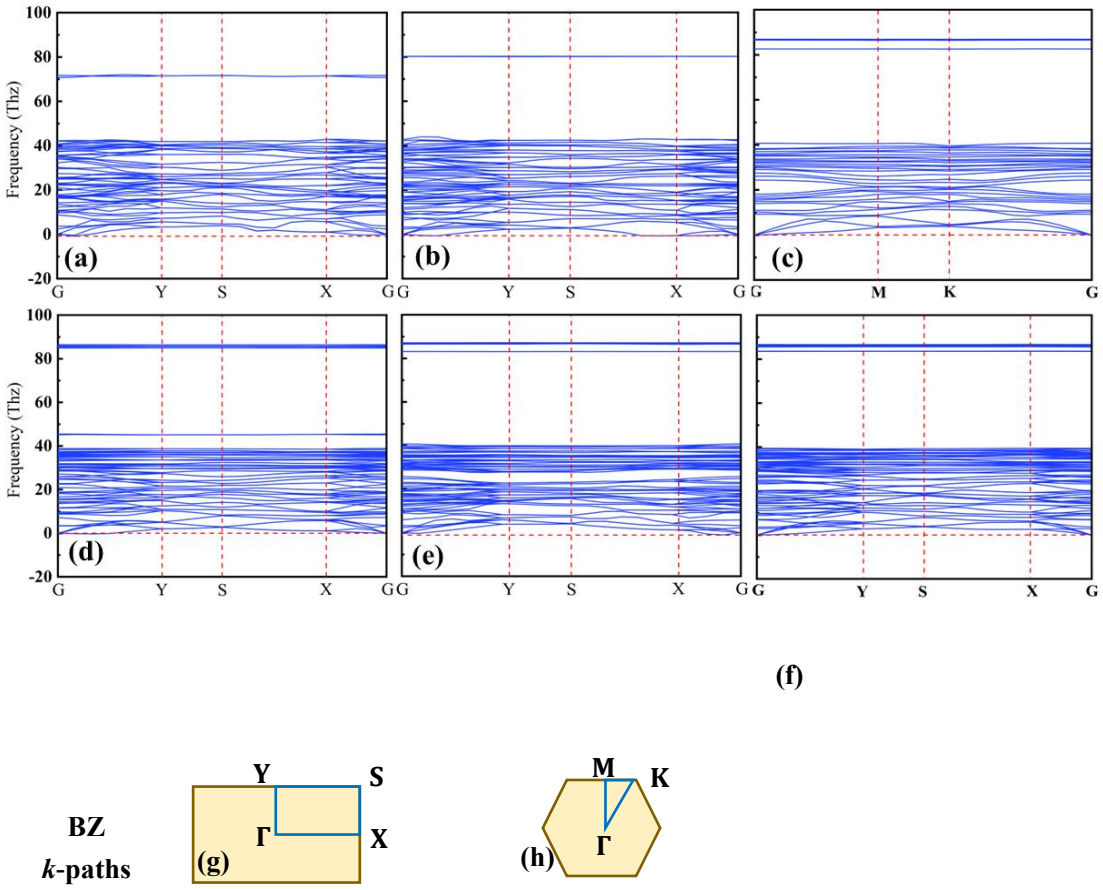

Fig. 3. (a-f) The phonon dispersions of the H_{α}^{1}-(C_3B), H_{ε}^{2}-(C_3B), H_{δ}^{3}-(C_3B), H_{λ}^{4}-(C_3B), H_{ε}^{5}-(C_3B) and H_{θ}^{6}-(C_3B); (g, h) represent two types of BZ to which the six belong.

After the structural relaxation of H_{α}^{1}-(C_3B)、H_{ε}^{2}-(C_3B)、H_{δ}^{3}-(C_3B)、H_{λ}^{4}-(C_3B)、H_{ε}^{5}-(C_3B) and H_{θ}^{6}-(C_3B), the structural symmetry changes to some extent. This is caused by the change of the bonding mode between C atom and B atom. When an H atom is suspended outside the C atom, the orbital hybridization mode changes from

sp^2 to sp^3 between C and B. The bonding energy of sp^3 hybrid is lower than that of sp^2. This can also be interpreted as the negative value of adsorption energy in Fig. 1(b). Table 2 lists the space groups, lattice constants and C-C bond lengths corresponding to each of the six hydrogenated stable configurations. It is noted that the length of C-C bond increases with the degree of hydrogenation, which is a direct effect of the change in hybrids orbitals. There are two BZ with six stable hydrogenation configurations, as shown in Fig. 3(g, h). different high k-points are determined according to this. Then, two k-point paths are determined, namely $\Gamma \to Y \to S \to X \to \Gamma$, $\Gamma \to M \to K \to \Gamma$. In order to further determine the dynamic stability of the above six hydrogenated C_3B, their phonon dispersion spectra were also calculated. Fig. 3(a-f) can reflect the phonon vibration information of the six hydrogenated C_3B lattices. The phonon spectra of the six structures have no virtual frequencies, which can judge the lattice stability of hydrogenated configurations H_{α}^{1}-(C_3B), H_{ε}^{2}-(C_3B), H_{δ}^{3}-(C_3B), H_{λ}^{4}-(C_3B), H_{ε}^{5}-(C_3B) and H_{θ}^{6}-(C_3B).[45]

Table 2. Space group, lattice constant and bond length corresponding to $\boldsymbol{H_{\alpha}^{1}}$-(C3B)、$\boldsymbol{H_{\varepsilon}^{2}}$-(C3B)、$\boldsymbol{H_{\delta}^{3}}$-(C3B)、$\boldsymbol{H_{\lambda}^{4}}$-(C3B)、$\boldsymbol{H_{\varepsilon}^{5}}$-(C3B) and $\boldsymbol{H_{\eta}^{6}}$-(C3B)

Configuration	Space Group	Lattice Constant (Å)		C-C Bond Distance (Å)
		a	b	
$\boldsymbol{H_{\alpha}^{1}-(C_3B)}$	CS-3	5.173	8.960	1.46/1.41/1.44
$\boldsymbol{H_{\varepsilon}^{2}-(C_3B)}$	C2-3	5.173	8.960	1.42/1.50/1.48
$\boldsymbol{H_{\delta}^{3}-(C_3B)}$	C1-1	5.173	5.173	1.58/1.52/1.42/1.43/1.5/1.54
$\boldsymbol{H_{\lambda}^{4}-(C_3B)}$	CS-3	5.173	8.960	1.57/1.58/1.51/1.38
$\boldsymbol{H_{\varepsilon}^{5}-(C_3B)}$	CS-3	5.173	8.960	1.53/1.65/1.49
$\boldsymbol{H_{\eta}^{6}-(C_3B)}$	C2-3	5.173	8.960	1.54/1.58/1.59/1.52

3.2 The bandgaps of hydrogenated C_3B

The surface functionalization can be enhanced by proper surface modification.[46] We choose hydrogen atoms to adsorb on C_3B surface to explore the changes and effects of its physical properties. As mentioned in Section 3.1, the incorporation of H atoms causes some changes in the original C3B structure, such as honeycomb type

and bonding mode. Specifically, with the increase of H atom doping, the sp^2 hybridized bonds around C atoms gradually transit to sp^3 hybridized bonds.[47] Thus, it can be predicted that the doping of impurity electrons will greatly effect the intrinsic properties of 2D materials. Fig. 4 (a-f) shows the energy bands of six stable hydrogenated configurations. Their bandgap values and types are: 0eV, 0.34eV (indirect, S-G), 0.56eV (indirect, G-K), 1.58eV (indirect, G-X), 0ev and 2.71eV (indirect, G-S). According to the above information, we can draw the following conclusions: hydrogen modification is an effective way to adjust C_3B band gap; as the number of external suspended H atoms gradually grows, valence band and conduction band widen and the band gap increases. To sum up, hydrogenation can directly effect the physical properties of monolayer C_3B and induce transition from metallicity to broad-bandgap semiconductor.

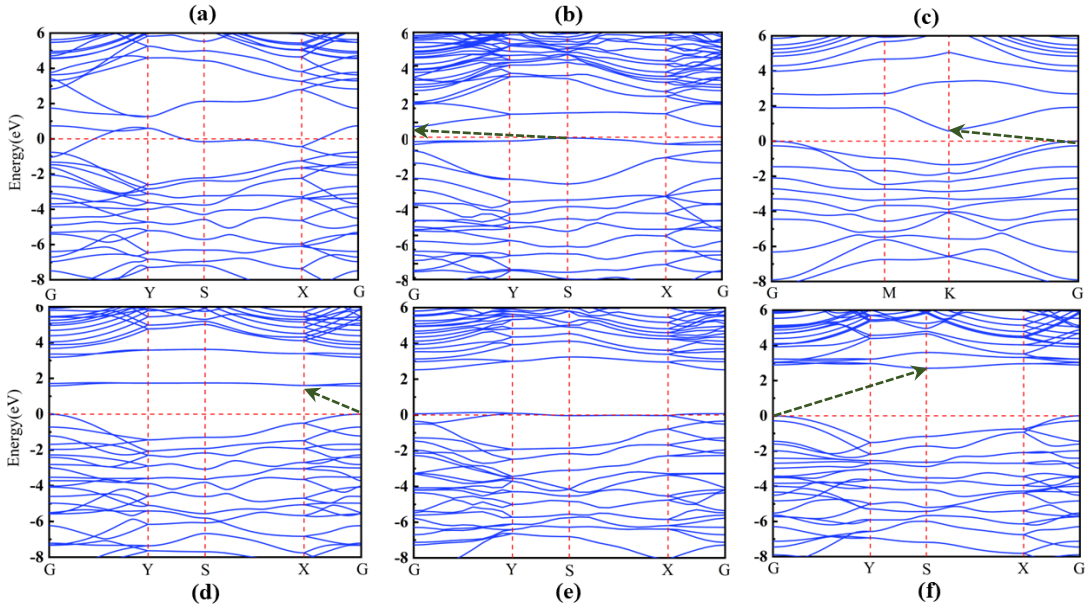

Fig. 4. (a-f) Band structures of the H_{α}^{1}-(C_3B), H_{ε}^{2}-(C_3B), H_{δ}^{3}-(C_3B), H_{λ}^{4}-(C_3B), H_{ε}^{5}-(C_3B) and H_{θ}^{6}-(C_3B), respectively.

In addition, the C_3B pristine structure contains a Carbon hexagon, in which C atoms are connected by π bonds. Next, we analyze these six adsorption situations one by one. For H_{α}^{1}-(C_3B), the complete carbon hexagon only adsorbs one H atom, and the outer electrons of the other C atoms cannot participate in bonding, so isolated

electrons will appear. These unpaired electrons are more likely to cross the Fermi surface, resulting metallicity in the material. Similarly, the quantity of H in H_{ε}^{5}-(C_3B) is odd. When the electrons pair into bonds, there must be isolated outer electrons left, which can illustrate the band gaps of H_{δ}^{3}-(C_3B), and H_{ε}^{5}-(C_3B).

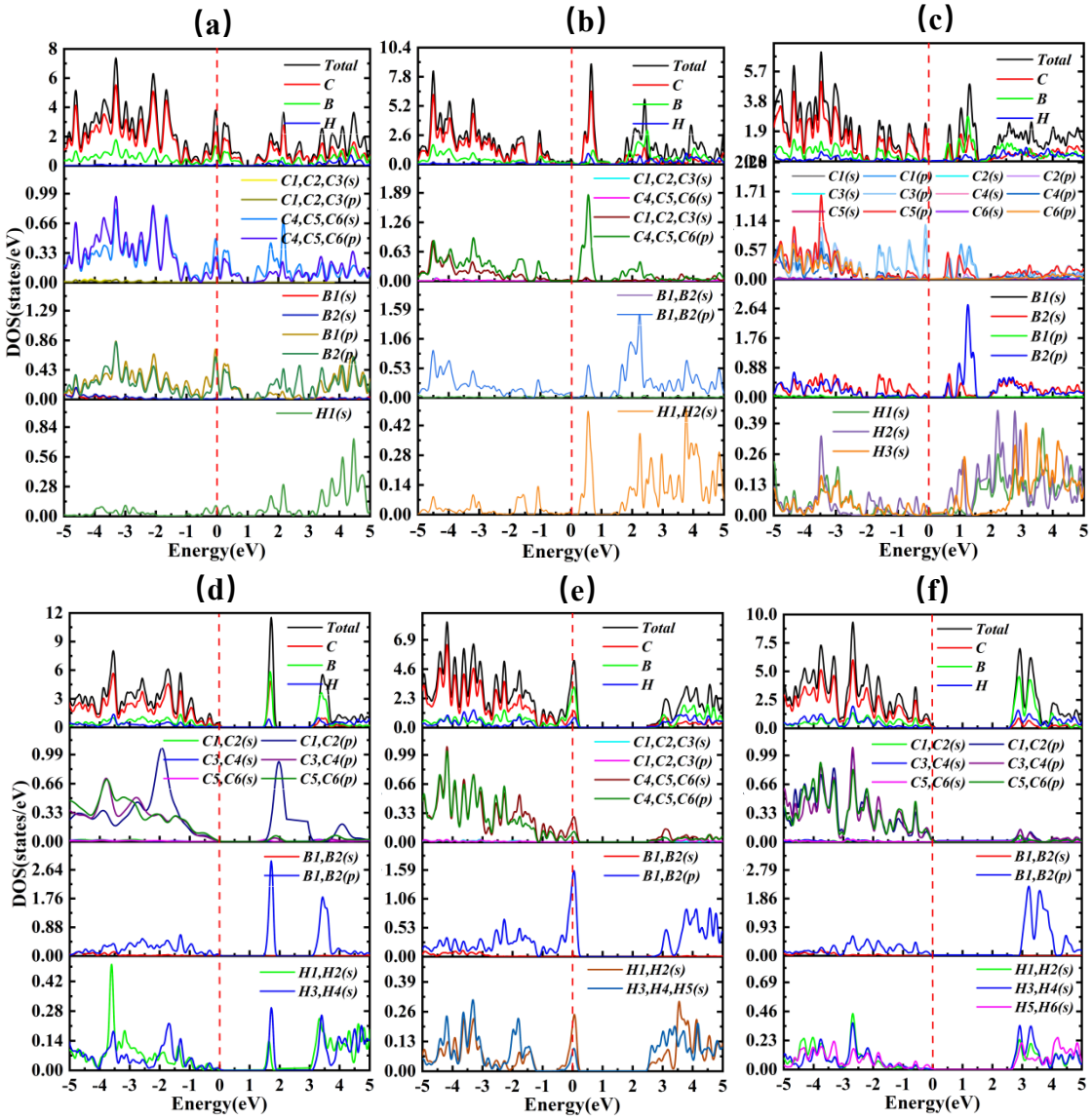

Fig. 5. (a-f) represents the TDOS and PDOS of the H_{α}^{1}-(C_3B), H_{ε}^{2}-(C_3B), H_{δ}^{3}-(C_3B), H_{λ}^{4}-(C_3B), H_{ε}^{5}-(C_3B) and H_{θ}^{6}-(C_3B), respectively. The dotted red line shows the position of the Fermi level.

Then, let's focus on H_{ε}^{2}-(C_3B), H_{λ}^{4}-(C_3B), and H_{θ}^{6}-(C_3B). An even number of H atoms are suspended outside them. The outer electrons are just bonded in pairs. Therefore, it is easy to show semiconductor properties as a whole. It is worth noting

that with the addition of H atoms, the C_3B configuration in the absolute two-dimensional plane begins to wrinkle, and there are more and more sp^3 hybrid orbitals, the degree of wrinkle becomes more and more obvious, and the band gap gradually increases (Eg (H_θ^6-(C3B))>Eg(H_λ^4-(C3B))>Eg(H_ε^2-(C3B)). Finally, it should be mentioned that the H_δ^3-(C_3B), with isolated electrons and more than half of the sp^3 orbitals hybridized C atoms, exhibits the properties of small bandgap semiconductors under the synergistic condition.

3.3 The electronic properties of hydrogenated C_3B

The bond state of the original C hexagon is broken and new electronic properties are excited. In order to further analyze the contribution of each orbital to the band structure, based on density functional theory, we calculate the electronic density of states of six stable hydrogenated structures. Fig. 5 shows the total density of states (TDOS) and partial density of state (PDOS) of the hydrogenated configuration. For each of the six graphs, looking from top to bottom, the first subgraph includes the TDOS of the C, N, H and all the atoms in a primitive cell, and the other subgraphs are the PDOS of C, N and H atoms. There are multiple atomic identifications of the same orbital in the PDOS, which means that there is more than one atom corresponding to the orbital. In brief, the PDOS of C in Fig. 5(a) is recorded as C1, C2, C3 (s), which means that there are three C atoms with the same contribution to DOS. And similar signs in Fig. 5(b-f) can be recognized and understood based on this.

According to the analysis of Fig. 5, the order of elements that contribute to the TDOS is: C, B, H. Firstly, analyze the case that the number of adsorbed H atoms is odd, as shown in Fig. 5(a), Fig.5(c) and Fig. 5(e). Although the electrons crossing the Fermi level mainly come from the p orbital of C and B, the contribution of H near the Fermi level cannot be ignored. This shows that when the number of H atoms adsorbed is an odd number, there will always be unbound isolated electrons left after the outer electrons are bonded in pairs. These lonely electrons readily cross the Fermi level. In

terms of structure, it is easier to show metallicity. Secondly, the number of adsorbed H atoms is even, as shown in Fig. 5(b), Fig.5(d) and Fig.5(f). Compared with the case of odd adsorption, all external electrons participate in bonding. Obviously, the contribution of H near the Fermi level is very little, so it is easier to show semiconductor properties. In addition, with the increase of the number of adsorbed H, there are more and more C atoms in sp^3 hybridization. The valence band in the band is getting lower and lower, so when the adsorption number is 6, the bandgap is the largest.

4. Optical properties of hydrogenated C_3B

Finally, we discuss the optical properties of C_3B due to the addition of H atom. Fig. 6 shows the optical absorption spectra of six stable adsorption configurations. According to the Fig. 6, six main absorption peaks of hydrogenated C_3B are gathered at about 100nm, and the position of secondary absorption peak is about 200-300nm. We focus on the main absorption peak located near 100nm. In order to observe the change of the main peak, Fig. 6(b) shows a local enlarged view with the wavelength at about 100nm. As can be seen from Fig. 6(b), with the proportion of hydrogen increases, the absorption intensity of the main peak decreases firstly and then increases. When the hydrogenation concentration is 50%, the main absorption peak splits and even divides into two. And the absorption range of the main peak appears dispersion, and the dispersion degree increases with the increase of hydrogenation degree as a whole. Let's turn our attention to the secondary absorption peak in the wavelength range of 200-300nm. The intensity change of the secondary peak is opposite to the main absorption peak, with the elevates of the number of H atoms adsorbed, the intensity of the secondary peak goes up firstly and then turns down. The maximum position of the secondary absorption peak just occurs when the hydrogenation ratio is 50%.

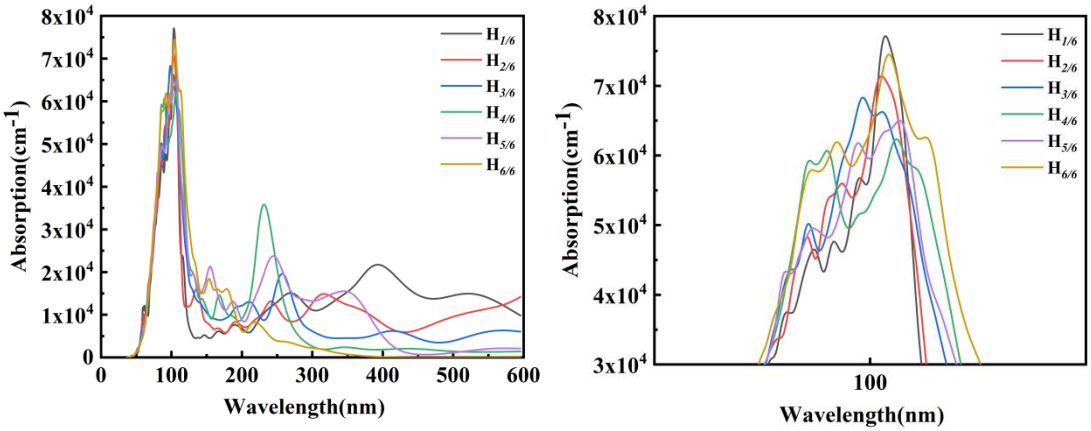

Fig. 6. Optical absorption spectra under six hydrogenation ratios; (b) partial enlarged drawing about 100 nm.

5. Conclusion

In this paper, 51 hydrogenated C3B structural models are designed, and six stable hydrogenated configurations (H_{α}^{1}-(C_3B), H_{ε}^{2}-(C_3B), H_{δ}^{3}-(C_3B), H_{λ}^{4}-(C_3B), H_{ε}^{5}-(C_3B) and H_{θ}^{6}-(C_3B)) are determined by adsorption energy and phonon dispersion spectra. Then, based on the first principle, the band structure, electronic properties and optical properties of hydrogenated C_3B are calculated and analyzed. The research results are summarized as follows:

(1) The adsorption of hydrogen atoms can adjust the bandgap of C_3B. When the number of adsorbed H is odd, there are unpaired isolated electrons in the structure, which are easy to jump over the Fermi level, so the structure is easy to show metallicity. Conversely, when the number of adsorbed h is even, the hydrogenated structure (H_{ε}^{2}-(C_3B), H_{λ}^{4}-(C_3B), H_{θ}^{6}-(C_3B)) appears as a semiconductor;

(2) The band edge position of C_3B structure is directly related to its hydrogenation ratio. The doping of hydrogen will effect the bonding mode of C in C_3B: sp^2 hybrid becomes sp^3 hybrid. This change directly leads to the energy reduction of valence band electrons near Fermi level and widen the bandgap;

(3) The degree of hydrogenation have an effect on the optical properties of C_3B. The main absorption peak and secondary absorption peak of C_3B are interrelated, which means one loss and the other gain.

In short, the theoretical calculation results show that hydrogenation provides a feasible way for the regulation of electronic properties of 2D materials such as C_3B. It is helpful to expand the practical application of 2D materials in the field of semiconductors and electronic devices.

Credit authorship contribution statement

Tong Liu, Dong Fang, Jie Ma and Qun Chao Fan conceived the idea. Tong Liu and Dong Fang performed the calculations. Tong Liu and Dong Fang wrote the manuscript and all authors contributed to revisions.

Declaration of competing interest

The authors declare that they have no known competing financial interests or personal relationships that could have appeared to influence the work reported in this paper.

Acknowledgements

This research is supported by the National Natural Science Foundation of China (Grant No. 61722507), the Fund for the Program of Science and Technology of Sichuan Province of China (Grant No. 2021ZYD0050), the Open Research Fund Program of the Collaborative Innovation Center of Extreme Optics (Grant No. KF2020003), and the National Undergraduate Innovation and Entrepreneurship Training Program of China (Grant No. S202210623081).

References

[1]. A. H. C. Neto, F. Guinea, N, M, R Peres et al., Rev. Mod. Phys. 81(1), 109 (2009)
[2]. B. Anasori, M. R. Lukatskaya, Y. Gogotsi., Nat. Rev Mater. 2(2), 1-17 (2017)
[3]. J. Pang, R. G. Mendes, A. Bachmatiuk et al., Chem. Soc Rev. 48(1), 72-133 (2019)
[4]. S. Z. Butler, S. M. Hollen, L. Cao et al., ACS nano. 7(4), 2898-2926 (2013)
[5]. D. Liu, W. Zhang, D. Mou et al., Nat. Commun. 3(1), 1-6 (2012)
[6]. M. M. Ugeda, A. J. Bradley, Y. Zhang et al., Nat. Phys. 12(1), 92-97 (2016)
[7]. C. Chen, H. Lv, P. Zhang et al., Nat. Chem. 14(1), 25-31 (2022)
[8]. W. Li, L. Kong, C. Chen et al., Sci. Bull. 63(5), 282-286 (2018)
[9]. A. J. Mannix, X. F. Zhou, B. Kiraly et al., Science. 350(6267) 1513-1516 (2015)
[10]. Y. Cai, Z. Bai, H. Pan, et al., Nanoscale. 6(3), 1691-1697 (2014)
[11]. J. Pei, J. Yang, X. Wang et al., ACS nano. 11(7), 7468-7475 (2017)

[12]. C. Shang, B. Xu, X. Lei et al., Phys. Chem. Chem. Phys. 20(32) 20919-20926 (2018)
[13]. J. Wang, F. Ma, W. Liang et al., Mater. Today. Phys. 2. 6-34 (2017)
[14]. L. Liu, Y. P. Feng, Z. X. Shen., Phys. Rev. B. 68(10), 104102 (2003)
[15]. M. C. Lemme, L. J. Li, T. Palacios et al., Mrs. Bull. 39(8), 711-718 (2014)
[16]. J. Zhou, Q. Wang, Q. Sun et al., Nano. Lett. 9(11), 3867-3870 (2009)
[17]. L. B. Shi, Y. Y. Zhang, X. M. Xiu et al., Carbon. 134, 103-111 (2018)
[18]. S. Yang, W. Li, C. Ye et al., Adv. Mater. 29(16), 1605625 (2017)
[19]. J. Mahmood, E. K. Lee, M. Jung et al., Nat. Commun. 6(1), 1-7 (2015)
[20]. S. Zhang, N. Wang, S. Liu et al., Nanotechnology. 27(27), 274001 (2016)
[21]. D. Voiry, H. Yamaguchi, J. Li et al., Nat. Mater. 12(9), 850-855 (2013)
[22]. Wang H, Lu Z, Xu S et al., P. Natl. Acad. Sci. 110(49), 19701-19706 (2013)
[23]. W. Hu, Z. Li, J. Yang., J. Chem. Phys. 138(12), 124706 (2013)
[24]. M. Bokdam, T. Amlaki, G Brocks et al., Phys. Rev. B. 89(20), 201404 (2014)
[25]. C. P. Lu, G. Li, K. Watanabe et al., Phys. Rev. L. 113(15), 156804 (2014)
[26]. K. Cheng, Y. Guo, N. Han et al., J. Mater. Chem. C. 5(15), 3788-3795 (2017)
[27]. A. Nourbakhsh, A. Zubair, M. S. Dresselhaus et al., Nano. Lett. 16(2) 1359-1366 (2016)
[28]. J. Wang, Z. Guan, J. Huang et al., J. Mater. Chem. A. 2(21), 7960-7966 (2014)
[29]. Y. Guo, K. Xu, C. Wu et al., Chem. Soc. Rev. 44(3), 637-646 (2015)
[30]. J. Deng, P. Ren, D Deng et al., Energ. Environ. Sci. 7(6), 1919-1923 (2014)
[31]. Y. Sun, F. Lei, S. Gao et al. Angew. Chem. Int. Edit. 125(40) 10763-10766 (2013)
[32]. Y. Sun, Z. Sun, S. Gao et al. Nat. Commun. 3(1), 1-7 (2012)
[33]. M. Makaremi, B. Mortazavi, C. V. Singh., J. Phys. Chem. C. 121(34), 18575-18583, (2017)
[34]. K. T. Chan, J. B. Neaton, M. L. Cohen., Phys. Rev. B. 77(23), 235430 (2008)
[35]. H. Sahin, F. M .Peeters., Phys. Rev. B. 87(8), 085423 (2013)
[36]. Y. Chen, Z. Wang, S. Chen et al., Nat. Commun. 9(1), 1-8 (2018)
[37]. C. Lin, X. Zhu, J. Feng et al., J. Am. Chem. Soc. 135(13), 5144-5151 (2013)
[38]. X. Li, J. Zhao, J. Yang., Sci. Rep. 3(1), 1-5 (2013)
[39]. S. J. Clark, M. D. Segall, C. J. Pickard et al., Z. Krist. Cryst. Mater. 220(5-6), 567-570 (2005)
[40]. M. D. Segall, P. J. D. Lindan, M. J. Probert et al., J. Phys. Condens. Mat. 14(11), 2717 (2002)
[41]. G. Kresse, D. Joubert., Phys. Rev. B. 59(3), 1758 (1999)
[42]. J. P. Perdew, K. Burke, M. Ernzerhof., Phys. Rev. Lett. 77(18), 3865 (1996)
[43]. A. V. Krukau, O. A. Vydrov, A. F. Izmaylov et al., J. Chem. Phys. 125(22), 224106 (2006)
[44]. Z. Wu, H. Zhang, J. Lin et al., Chem. Phys. 2020, 528: 110471.
[45]. P. Giannozzi, S. De Gironcoli, P. Pavone et al., Phys. Rev. B. 43(9), 7231 (1991)
[46]. K. Huang, Z. Li, J. Lin et al., Chem. Soc. Rev. 47(14), 5109-5124 (2018)
[47]. X. Niu, X. Bai, Z. Zhou et al., ACS Catal. 10(3), 1976-1983 (2020)